Strangeness production time and the K^+/π^+ horn

Boris Tomášik[12] and Evgeni E Kolomeitsev[3]

[1] Fakulta prírodných vied, Univerzita Mateja Bela, Tajovského 40, 97401 Banská Bystrica, Slovakia
[2] Ústav vedy a výskumu, Univerzita Mateja Bela, Cesta na amfiteáter 1, 97401 Banská Bystrica, Slovakia
[3] University of Minnesota, School of Physics and Astronomy, 116 Church Street SE, Minneapolis, 55455 Minnesota, USA

February 9, 2008

Abstract. We construct a hadronic kinetic model which describes production of strange particles in ultrarelativistic nuclear collisions in the energy domain of SPS. We test this model on description of the sharp peak in the excitation function of multiplicity ratio K^+/π^+ and demonstrate that hadronic model reproduces these data rather well. The model thus must be tested on other types of data in order to verify the hypothesis that deconfinement sets in at lowest SPS energies.

PACS. 25.75.-q Relativistic heavy-ion collisions – 25.75.Dw Particle and resonance production

1 Introduction

The central issue in studies with ultrarelativistic heavy ion collisions is to map the phase diagram of strongly interacting matter. From lattice QCD and numerous investigations with effective models we know that at high enough energy density hadronic matter melts to a phase where quarks and gluons are the relevant degrees of freedom. Data on jet quenching at RHIC energies indicate very clearly that such a deconfined phase has been produced there [1,2,3,4]. This does not, however, answer the question *where is the threshold* for deconfinement.

In order to find the minimum collision energy at which the hadronic description of collision dynamics turns inadequate, a natural choice is to study various excitation functions, i.e. dependences of quantities on the collision energy. The expectation here is that a change of the quality of the system would demonstrate itself as a non-monotonic dependence of some excitation function. A set of interesting excitation functions has been observed in the energy scan at the SPS. These include: i) a sharp peak at projectile energy 30 AGeV of the ratio of positive kaon to pion multiplicities ("the horn"); ii) a change in the slope of number of produced pions per participating nucleon ("the kink"); and iii) a plateau in the excitation function of kaon mean p_t which is otherwise increasing function of the collision energy ("the step") [5,6]. In addition to this, event-by-event fluctuation of the K/π multiplicity ratio grows when the collision energy is lowered and reaches maximum at lowest SPS energies, though we have to note that there are no data at lower energies from AGS.

These observed features possibly indicate qualitative changes of the system. A possible explanation is that they are caused by the onset of deconfinement. Such a *positive* reasoning is insufficient, however, for claims of this kind

of discovery. In fact, one would have to demonstrate that any purely hadronic description of the data fails. In this paper we embark on such a programme and address one of the excitation functions: the horn.

Currently, the data have been addressed in many different approaches. Transport codes generally fail in reproducing some of the observed multiplicities as functions of collision energy and thus fail in ratios [7]. A three-fluid hydrodynamic simulation does not correctly reproduce the multiplicity of negative pions [8]. Statistical hadronisation model leads to a broad peak of the K^+/π^+ ratio as a function of collision energy which is put in connection with transition from baryon-dominated to meson-dominated entropy [9]. The peak is much broader than observed, however. Data are better reproduced in a statistical hadronisation fit in which strange species are suppressed with respect to chemical equilibrium by a strangeness suppression factor [10]. A question appears then, what is the mechanism leading to the particular value of strangeness suppression factor?

The data are successfully interpreted in framework of the so-called Statistical Model of the Early Stage (SMES) [11]. The model predicts first order phase transition and the existence of mixed phase, which sets in about the beam energy of 30 AGeV. Another important ingredient of the model is the assumption of an immediate chemical equilibration of the primordial production of quanta. A non-equilibrium kinetic calculation reproducing the data which also includes first order phase transition has been proposed recently [12].

We shall construct hadronic non-equilibrium kinetic model and try to reproduce the peak in the ratio of multiplicities K^+/π^+. It will be shown that these data can be interpreted in framework of such a model and there-
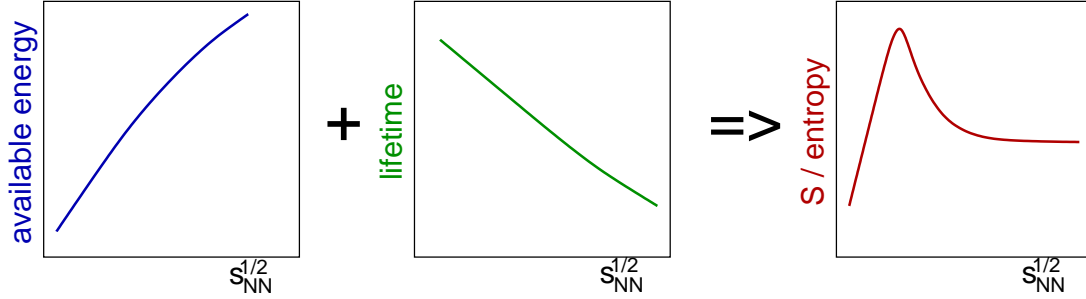
Fig. 1. (colour online) If energy available for production of strange particles increases with collision energy while the lifetime of fireball decreases with increasing collision energy, these two excitation functions might combine into a peak in strangeness-to-entropy ratio as a function of collision energy. The ratio of strangeness to entropy is experimentally accessible through the ratio of positive kaon to pion multiplicity.

fore hadronic description must be tested on other types of data until it can be safely ruled out.

2 Strangeness production: cartoon description

Strange particles are produced in nucleon-nucleon reactions, though in smaller fraction to non-strange ones than in nuclear collisions. We shall assume that the corresponding surplus of strange particles is produced in secondary reactions of hadrons generated in nuclear collisions. Then, two aspects are important for strangeness production: available energy and time.

The available energy is microscopically represented through energy density. At typical momenta of particles in the considered environment, many secondary reactions run close to the threshold of kaon and hyperon production. In such a case, production rates depend strongly on incoming momenta and densities of reactants, which both depend on temperature (if it is defined). Higher energy density (and temperature) implies higher production rates.

Since strangeness is under-represented with respect to chemical equilibrium in nucleon-nucleon collisions, its amount in the system will increase with time until it saturates. Thus longer total lifespan of the system would also mean larger relative amount of strange particles. This picture becomes slightly more complicated in an expanding and cooling system, but the simple assumption that the amount of strange particles grows with time is good enough for the cartoon-like explanation offered in this section.

Now we can imagine the following explanation of the K^+/π^+ horn (Fig. 1): the energy density within the system which is available for production of strange particles is an increasing function of the collision energy. We could also assume that the total lifespan of the fireball decreases as the collision energy grows. These two features might be combined in such a way, that the strangeness-to-entropy ratio—which is basically measured by the K^+/π^+ ratio— shows a sharp peak as it is indeed observed. In the next Section we shall describe this model in more technical terms.
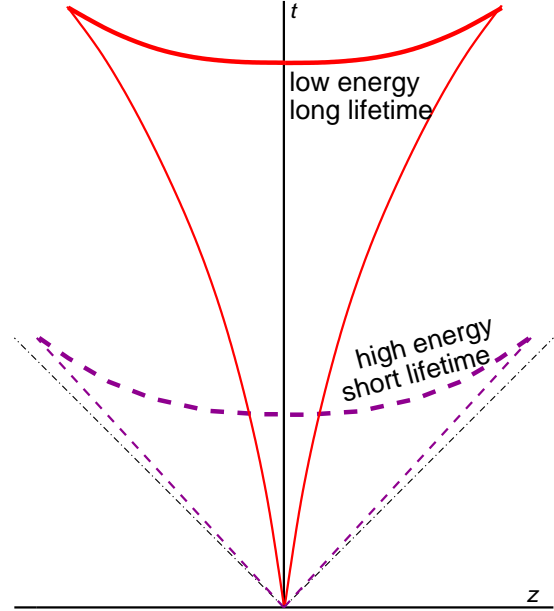

Fig. 2. (colour online) Evolution scenarios and freeze-out hypersurfaces in a space-time diagram for fireballs created at lower collision energy with strong stopping and re-expansion (solid line), and higher collision energy in nuclear transparency regime (dashed line). Longer lifetime of a fireball does not necessarily imply larger extent in longitudinal direction.

The assumed dependence of the total lifespan on collision energy may result from an interplay between stopping and subsequent accelerated expansion. At low collision energy we expect strong slowing down of the incident nucleons. Then the system needs time in order to build up expansion from pressure and to expand up to the breakup density. At higher collision energy stopping is weaker and the incident nucleons continue longitudinal movement. Thus expansion is present from the first moments of fireball evolution and it takes shorter time to get to the critical breakup density. Let us also stress that the assumption of shorter lifespan at higher collision energy does *not* clearly contradict any existing data. It does *not* imply larger longitudinal extent of the fireball and a larger freeze out volume (Fig. 2). Hence, it also does not

necessarily lead to higher multiplicity at lower collision energy. In fact, the correspondence between lifetime and the longitudinal size is model-dependent and one usually thinks about Bjorken boost-invariant expansion [13] when making such a connection, but this is not the generally applicable hydrodynamic solution.

3 The kinetic model

We shall construct a kinetic model for the production of strange particles. Such a calculation requires knowledge of the local densities of reacting species. This is naturally provided in so-called hydro-kinetic or flavour kinetic models [14,15,16,17,18,19]. It is known, however, that most hydrodynamic and kinetic models have problems with reproducing the space-time extent of the fireball measured by femtoscopy. Therefore, we shall not use such a model in order to calculate the space-time evolution of the fireball. Instead, we will parametrise the evolution of the density. In this way, we do not couple our approach directly to the microscopic structure of the matter or to its equation of state. On the other hand, we can choose many different parametrisations of the fireball evolution and check which of them might lead to results consistent with data. Our ansatzes for these parametrisation will be constructed with one eye on femtoscopy data and hadronic spectra.

As we are now only interested in *ratios* of multiplicities it will be sufficient to calculate the *densities* of individual species in the kinetic approach. For densities of kaons with positive strangeness we derive

$$\frac{d\rho_K}{d\tau} = \frac{d}{d\tau}\frac{N_K}{V} = -\frac{N_K}{V}\frac{1}{V}\frac{dV}{d\tau} + \frac{1}{V}\frac{dN_K}{d\tau}. \qquad (1)$$

Notice that the first term on the right hand side $1/V\, dV/d\tau$ actually includes the expansion rate which will follow from our assumption for density evolution. The second term includes the rate of change of the number of kaons. It can be divided into two contributions: production rate and annihilation rate. The former stands for all processes which produce a kaon while the latter includes processes which destroy kaons. They are determined from cross-sections of these processes and evolved densities. Thus the master equation for kaon density reads

$$\frac{d\rho_K}{d\tau} = \rho_K\left(-\frac{1}{V}\frac{dV}{d\tau}\right) + \mathcal{R}_{\text{gain}} - \mathcal{R}_{\text{loss}}. \qquad (2)$$

3.1 Production and annihilation

Densities of K^+, K^0, K^{*+}, and K^{*0} are evolved according to eq. (2). Here we always assume that all particles keep their vacuum properties. The gain term has in our treatment basically two types of contributions

$$\mathcal{R}_{\text{gain}} = \sum_{ijX}\langle v_{ij}\sigma_{ij}^{KX}\rangle\frac{\rho_i\rho_j}{1+\delta_{ij}} + \rho_{K^*}\Gamma_{K^*}, \qquad (3)$$

where the sum goes over two-to-N processes leading to production of kaons and the second term is for K^* decay into K. The term in angular brackets is cross-section of a process multiplied with *relative* velocity of the reacting species and averaged over the distribution of relative velocities. For the sake of this averaging we always assume thermal distribution of velocities. The annihilation term is obtained in a similar way

$$\mathcal{R}_{\text{loss}} = \sum_{iX}\langle v_{Ki}\sigma_{Ki}^X\rangle\frac{\rho_K\rho_i}{1+\delta_{Ki}}. \qquad (4)$$

In a real calculation, it is impossible to include all processes that create or destroy a kaon. Only the most important ones are included here:

- Associated production of kaon and a hyperon in reactions of $\pi N \leftrightarrow KY$ and $\pi\Delta \leftrightarrow KY$. In order to keep the detailed balance, these reactions are included in both directions, i.e., creating and annihilating kaons.
- Meson-meson reactions of $\pi\pi$, $\pi\rho$, and $\rho\rho$ are also included in both directions.
- K^* production from πK collisions and its decay.
- Reactions of $\pi Y \leftrightarrow K\Xi$.
- Baryon-baryon reactions which lead to kaons in the final state are included only in the gain term.

For details of parametrisations of all the used cross-sections we refer the reader to [20]. Note that no reactions involving antibaryons have been taken into account. Since nuclear collisions create a *baryon rich* environment the error due to this simplification is reasonable. It is largest at the highest SPS energy (we do not apply this model to higher energies) where we estimate it around 10%.

Other species than kaons with $S > 0$ are not treated explicitly in the kinetic approach. Chemical reactions changing their numbers are swift and therefore we can assume that non-strange species are kept in chemical equilibrium during the whole evolution. For species with $S < 0$—which include K^- and $\bar{K}^0$ as well as Λ, Σ, Ξ, and Ω—we assume that they are in *relative* chemical equilibrium, i.e., that all the strange quarks are distributed in the system according to principle of maximum entropy although their total number is given by the number of produced strange antiquarks contained in kaons.

3.2 The ansatz for expansion

We shall assume that the evolution of fireball densities consists basically from two periods: initial accelerating period and later scaling expansion with power-law dependence of density on time. Since baryon number is a conserved quantum number, evolution of baryon density actually determines the expansion of the volume. We write it as

$$\rho_Q(\tau) = \begin{cases} \rho_{Q0}(1 - a\tau - b\tau^2)^\delta & : \tau < \tau_s, \\ \frac{\rho'_{Q0}}{(\tau-\tau_0)^\alpha} & : \tau \geq \tau_s, \end{cases} \qquad (5)$$

where ρ_{Q0}, a, b, ρ'_{Q0}, τ_0, τ_s, α and δ are parameters which can be tuned. They can be put in relation to the total lifetime, initial density, initial density decrease etc. [20]. The

subscript Q stands for any conserved quantum number; in our treatment we explicitly take care of baryon number and the third component of isospin. This parametrisation is motivated by simplicity: at the beginning the simplest way of encoding the acceleration of expansion is through second order polynomial, while the power law in the end is commonly used in analysis of correlation radii.

The energy density is parametrised in a similar way

$$\varepsilon(\tau) = \begin{cases} \varepsilon_0(1 - a\tau - b\tau^2) : \tau < \tau_s \\ \dfrac{\varepsilon_0'}{(\tau - \tau_0)^{\alpha/\delta}} \quad\quad : \tau \geq \tau_s \end{cases}, \quad (6)$$

so the parameter δ represents a simple way of choosing the equation of state.

By exploring a range of parameters we can tune our parametrisation between the well known Bjorken [13] and Landau [21] hydrodynamic solutions of fireball expansion.

3.3 Initial and final conditions

Since kaons are also produced in nucleon-nucleon interactions, there must be some initial kaon density due to primordial kaon production in collisions of incident nucleons. It is estimated [20] from a compilation of kaon production data in nucleon-nucleon collisions [22].

Then, species containing strange quarks must balance the strange antiquarks such that the total strangeness vanishes. Among themselves they are in relative equilibrium.

The most important choice is that of the total lifetime of the fireball and the initial energy density. This, together with the final state densities, basically determines the whole evolution scenario.

The energy density and number densities in the final state, i.e., at the end of parametrisations (5) and (6), are chosen so that they correspond to the measured values. The values from experiment were calculated from results of chemical freeze out fit with a statistical model [10].

Thus the construction of our model guarantees that we end up with the correct final state values of energy density, baryon density, and the density of third component of isospin. It still does not guarantee, however, the correct K^+ abundance, as kaons are produced kinetically. But once we get the right amount of kaons, together with the densities this implies the correct value of temperature and chemical potentials. Consequently, the whole chemical composition is correct in such a case.

3.4 Kaon and Λ production

From what has been said it should be now easy to understand how the production of kaons, antikaons, and lambdas is steered by different knobs. This is important as we shall fit the ratios of their multiplicities to pion multiplicity. The amount of kaons is mainly given by the lifetime of the whole system and also by the initial energy density. The strange quarks are distributed—in a simplified picture for the sake of this explanation—among antikaons
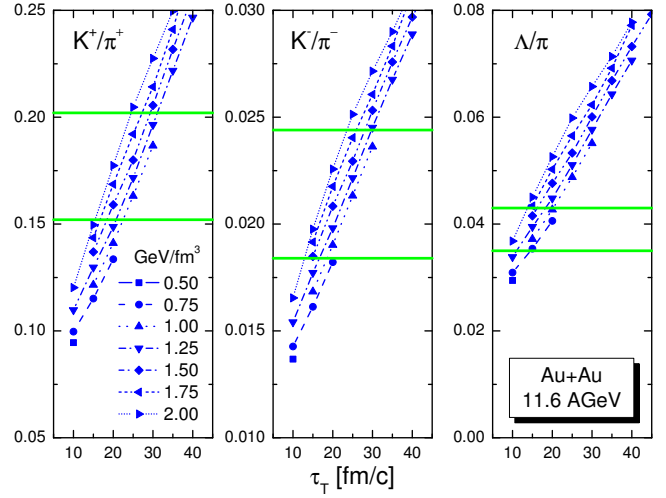

Fig. 3. (colour online) The ratios of multiplicities K^+/π^+ (left panel), K^-/π^- (middle), and Λ/π (right) calculated in scenarios with various initial energy densities and total lifetimes of the fireball for Au+Au collisions at projectile energy 11.6 AGeV. The plots show dependence of the ratios on the *total* lifetime of the fireball. Different curves correspond to different initial energy densities. Horizontal lines indicate the 1σ intervals around the measured values.

and hyperons. The distribution of these quarks among antikaons and hyperons is given in relative chemical equilibrium by the temperature and baryonic chemical potential.

In summary: lifetime determines the amount of kaons, and subsequently temperature specifies how many antikaons and hyperons there will be.

4 Results

We have run our hadronic kinetic model for various sets of model parameters for Au+Au collisions at projectile energy 11.6 AGeV (highest AGS energy) and then Pb+Pb collisions at 30, 40, 80, and 158 AGeV (SPS), so that we safely cover the region where the K/π horn appears. For each value of initial energy density and the total lifetime we evolve kaon densities. At the end, we add the feed-down to kaons and pions due to resonance decays. (Details of this procedure can be found in [20].)

Some selected results are shown in Figs. 3, 4, and 5. In general, we observe that the resulting ratios mainly depend on the total lifetime and less so on the initial energy density. It seems that the data values can be reproduced with rather reasonable lifetimes, though somewhat longer than one would infer from analysis of correlation radii based on Bjorken hydrodynamic solution.

In order to make our comparison with data more quantitative, we calculate for each set of results

$$\chi^2 = \sum_i \frac{(d_i - t_i)^2}{\sigma_i^2}, \quad (7)$$

where t_i, d_i, and σ_i are the calculated and measured values and experimental error, respectively. For all calculated
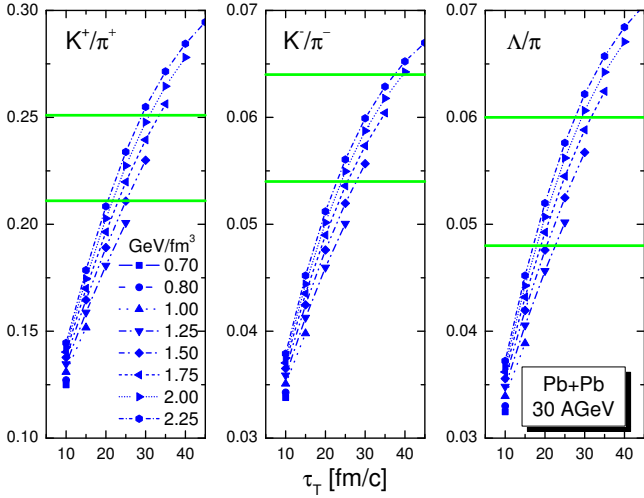
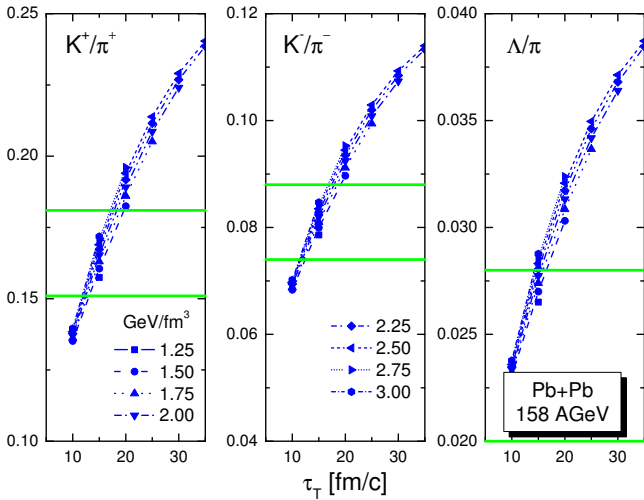**Fig. 4.** (colour online) Same as Fig. 3 but for Pb+Pb collisions at projectile energy 30 AGeV.

Fig. 5. (colour online) Same as Fig. 3 but for Pb+Pb collisions at projectile energy 158 AGeV.

scenarios the values of χ^2 are summarised in Fig. 6. We observe that the maximum of K^+/π^+ ratio of multiplicities as a function of collision energy is basically translated into a maximum lifetime of the fireball for the best reproduction of data, although such a conclusion is not statistically significant. One could speculate if it is connected with long total lifetime due to a soft point in the equation of state which would appear close to the phase transition.

On the other hand, based on comparison with data one neither can exclude that the total lifetime of the fireball does not increase and rather decreases when the collision energy grows. In order to demonstrate this we choose for each collision energy one set of parameters, and show results calculated with those parameters compared to data in Fig. 7. The lifetimes and initial energy densities from the used parameter sets are collected in Table 1.

From the table we also see that the final state temperature which we obtain does not differ much from the result of chemical freeze-out analysis. Hence, we conclude
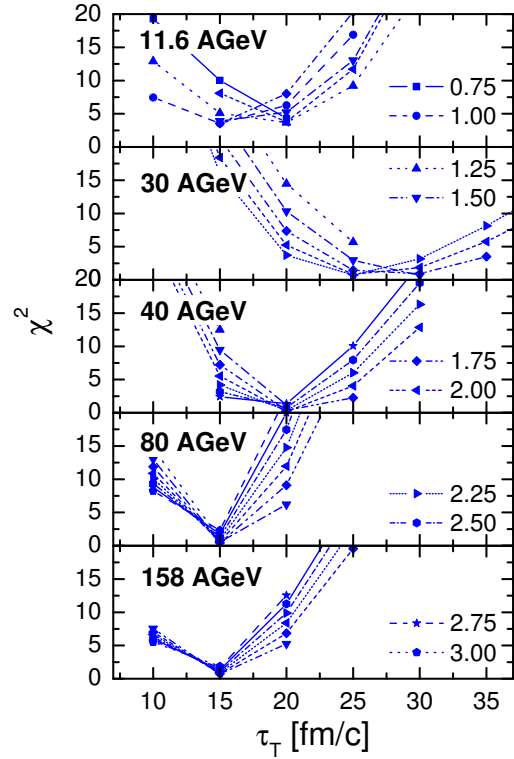

Fig. 6. (colour online) Quantity χ^2 defined in eq. (7) evaluated for results from all simulations. Plots show the dependence on total lifetime and different curves correspond to different initial energy densities.
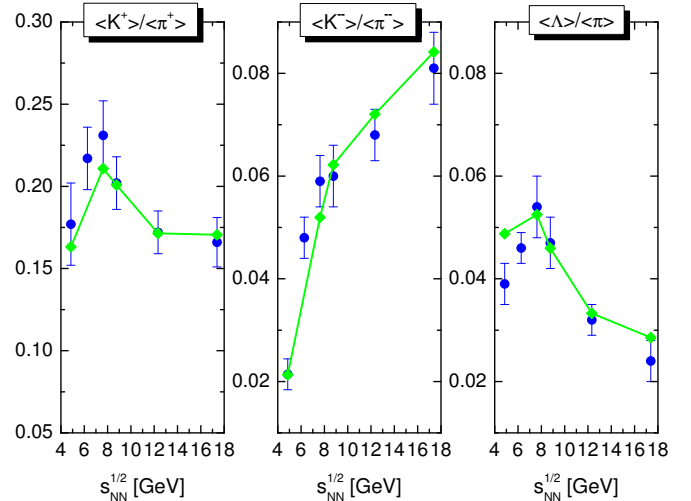

Fig. 7. (colour online) Comparison of selected results of our simulations with data. Plotted are excitation functions of multiplicity ratios of K^+/π^+ (left panel), K^-/π^- (middle), and Λ/π (right). Data points from [6].

that not only kaon production, but the whole calculated chemical composition is correct.

Table 1. Initial energy densities and total lifetimes from parameter sets which were used in calculations leading to results shown in Fig. 7. In the lower portion of the table, T_f is the final state temperature obtained in our simulations and T the temperature from the analysis of chemical freeze-out [10].

E_{beam} [AGeV]	11.6	30	40	80	158
ε_0 [GeV/fm^3]	1	1.5	2	2.25	2.75
τ_T [fm/c]	25	25	20	15	15
T [MeV]	118.1	139.0	147.6	153.7	157.8
T_f [MeV]	114.7	134.1	143.3	149.3	153.6

5 Conclusions

The actual aim in search for the onset of deconfinement is to falsify hadronic description of data. This has not been accomplished here. Our hadronic kinetic model was able to describe the excitation function of the multiplicity ratios K^+/π^+, K^-/π^-, and Λ/π. It requires, certainly at least for beam energies above 30 AGeV, that the lifetime of fireball decreases as the energy of collisions grows.

So far, we only checked our model against one type of data. In order to verify or falsify it, it will have to be tested on other interesting excitation functions mentioned in the Introduction as well as the "standard" data like, transverse momentum spectra and correlation radii. Since we make statements about the whole evolution of the fireball, it seems important to calculate our prediction for dilepton spectra which are produced during the whole evolution.

Finally, so far we have put aside the question of how the evolution which we parametrised can result from microscopic structure of the matter. If the model passes all data tests, this question will have to be addressed.

Acknowledgements

References

1. I. Arsene *et al.* [BRAHMS collab.], Nucl. Phys. A **757** (2005) 1
2. B.B. Back *at al.* [PHOBOS collab.], Nucl. Phys. A **757** (2005) 28
3. J. Adams *et al.* [STAR collab.], Nucl. Phys. A **757** (2005) 102
4. C. Adcox *et al.* [PHENIX collab.] Nucl. Phys. A **757** (2005) 184
5. S.V. Afanasiev *et al.* [NA49 collab.], Phys. Rev. C **66** (2002) 054902
6. B. Lungwitz for the NA49 collab., AIP Conf. Proc. **828** (2006) 321
7. E.L. Bratkovskaya *et al.*, Phys. Rev. C **69** (2004) 054907
8. Yu.B. Ivanov, V.N. Russkikh, V.N. Toneev, Phys. Rev. C **73** (2006) 044904
9. J. Cleymans, H. Oeschler, K. Redlich, S. Wheaton, Phys. Lett. B **615** (2005) 50
10. F. Becattini, M. Gaździcki, A. Keränen, J. Manninen, R. Stock, Phys. Rev. C **69** (2004) 024905
11. M. Gaździcki, M.I. Gorenstein, Acta Phys. Pol. B **30** (1999) 2705
12. J.K. Nayak, J.e. Alam, P. Roy, A.K. Dutt-Mazumder, B. Mohanty, Acta Phys. Slov. **56** (2005) 27
13. J.D. Bjorken, Phys. Rev. D **27** (1983) 140
14. P. Koch and J. Rafelski, Nucl. Phys. A **444** (1985) 678
15. P. Koch, B. Müller, J. Rafelski, Phys. Rep. **142** (1986) 167
16. J.I. Kapusta and A. Mekjian, Phys. Rev. D **33** (1986) 1304
17. H.W. Barz, B.L. Friman, J. Knoll, H. Schulz, Nucl. Phys. A **484** (1988) 661
18. H.W. Barz, B.L. Friman, J. Knoll, H. Schulz, Nucl. Phys. A **519** (1990) 831
19. G.E. Brown, C.M. Ko, Z.G. Wu, L.H. Xia, Phys. Rev. C **43** (1991) 1881
20. B. Tomášik and E.E. Kolomeitsev, nucl-th/0512088
21. L.D. Landau, Izv. Akad. Nauk SSSR, Ser. Fiz., **17** (1953) 51
22. M. Gaździcki and D. Röhrich, Z. Phys. C **71** (1996) 55.